Journal of Applied Electrochemistry **31**: 1025–1031, 2001.
© 2001 *Kluwer Academic Publishers. Printed in the Netherlands.*

Iron(III) tetramethoxyphenylporphyrin (FeTMPP-Cl) as electrocatalyst for oxygen reduction in direct methanol fuel cells

G.-Q. SUN, J.-T. WANG, S. GUPTA and R.F. SAVINELL*
Department of Chemical Engineering and Ernest B. Yeager Center for Electrochemical Sciences, Case Western Reserve University, Cleveland, OH 44106-7217, USA
*(*author for correspondence)*

Received 22 August 1997; accepted in revised form 9 May 2001

Key words: carbon supports, oxygen cathodes, PBI, PEM

Abstract

Iron(III) tetramethoxyphenylporphyrins (FeTMPP-Cl) adsorbed on high-area carbons were heat treated in an inert atmosphere at various temperatures ranging from 200–1000 °C to produce catalysts for the electroreduction of oxygen in acid electrolytes. It was found that the specific surface area of the FeTMPP-Cl/C catalysts linearly decreases with increase of the FeTMPP-Cl loading on RB carbon. The electrical resistivity of the catalyst decreases with the increase of heat treatment temperature in the range of 200 to 800 °C, then it increases beyond 800 °C. The results obtained with elemental analysis, FTIR spectroscopy and XPS techniques indicate that the onset temperature for partial decomposition for the FeTMPP chelate occurs at temperatures of about 400–500 °C. The surface concentrations of both iron and nitrogen on the carbon support increase as the heat treatment temperature increases, and the maximum occurs at 700 °C. Some possibilities about the nature of active sites in the catalysts are discussed.

1. Introduction

Direct methanol fuel cells (DMFC) using a solid polymer electrolyte, such as Nafion® and polybenzimidazole, offer an opportunity for high efficiency, small volume and lightweight energy conversion devices [1, 2]. One of the challenges with DMFC is that the cathode, which typically contain platinum-based electrocatalysts, is adversely affected by the presence of methanol which diffuses through the polymer electrolyte membrane from the anode. Mixed-potential and poisoning effect occurs at the cathode that leads to cathode performance decline. A possible approach to overcome this problem is to use methanol tolerant oxygen reduction electrocatalysts which are inactive toward methanol oxidation.

Since Jasinski [3] first reported the effectiveness of metallophthalocyanines as catalysts for the cathodic reduction of oxygen in alkaline solutions, many efforts have been directed toward finding materials which exhibit high activity for electrochemical oxygen reduction [4–11]. These catalysts were prepared by the dispersion of certain transition metal macrocycles on high area carbons followed by a heat treatment in an inert atmosphere at temperatures ranging from 600 to 1000 °C. A number of researchers reported that improved oxygen reduction activity and stability were observed for a variety of porphyrins and phthalocyanines adsorbed on carbon and heat treated at 600–800 °C [12–18]. It was suggested that the N_4–Me moiety of the macrocycles is the structure associated with the high activity of the heat-treated materials [12, 13]. This explanation was largely adopted by other workers in this field. However, no general agreement on the nature of the active site of the catalysts and the configuration of macrocycles after heat-treatment exists so far [14, 15]. These active oxygen reduction catalyst have been shown to be tolerant to the presence of methanol [15, 17, 18].

In this work, some basic data of physical behaviors of iron(III) tetramethoxyphenylporphyrin (FeTMPP-Cl) supported on high area carbons were obtained from the measurements of specific surface area and electrical resistivity for FeTMPP-Cl/C catalysts before and after heat treatment at various temperatures. Elemental analysis and spectroscopic techniques, such as X-ray photoelectron spectroscopy (XPS) and Fourier transform infrared (FTIR) spectroscopy, were also used to provide insight into the molecular structure of FeTMPP chelate on carbon supports before and after heat treatments at various temperatures. The catalytic activity for oxygen reduction was examined via conventional gas diffusion electrode under fuel cell operating condition.

2. Experimental details

2.1. *Catalyst preparation*

The iron(III) tetramethoxyphenylporphyrin (FeTMPP-Cl) was obtained from Aldrich Chemical Company and was used without further purification. The high-area carbons were undeashed RB carbon (Calgon Corp., Pittsburgh, PA) and Black Pearls 2000 (Cabot Corp., Billerica, MA).

Catalysts were prepared by dissolving an amount of FeTMPP-Cl in acetone, mixing a specified amount of carbon black and agitating the mixture by using a magnetic stirrer for about 20 h and then filtering rapidly through a nuclepore polycarbonate membrane (1 μm pore side). The concentration of the macrocycle in the filtrate was measured spectrophotometrically and thus the amount of the macrocycle adsorbed on the carbon was calculated. The solid samples were then heat treated in a horizontal tube furnace at 800 °C for 2 h under continuous flow of purified argon (Metheson, H.P. grade), and allowed to cool while still under flowing argon. The catalyst samples for the heat temperature effect study were prepared by the same way but heat treated at different temperatures, 200 °C (HT 200), 400 °C (HT 400), 600 °C (HT 600), 700 °C (HT 700), 800 °C (HT 800) and 1000 °C (HT 1000), for 2 h in argon atmosphere. To increase the FeTMPP-Cl loading, further amounts of FeTMPP-Cl were reabsorbed on heat-treated catalyst/carbon materials and the resulting material was reheat-treated at 800 °C for 2 h. The catalyst/carbon samples with 29.6 wt % and 36.9 wt % FeTMPP-Cl on RB carbon were obtained by repeat the absorption and heat treatment process two and four times, respectively.

2.2. *Specific surface area measurement*

The specific surface areas of the carbons, FeTMPP chelate and the carbon supported FeTMPP-Cl catalysts were measured by conventional BET method at room temperature. The Quantasorb Jr including a Quantector and a Flow Controller (Quanta Chrome Inc.) was used for those measurements.

2.3. *Resistivity measurement*

A schematic of the test hardware for measuring electrical resistivity of carbon and catalysts is shown in Figure 1. The body of the test cell was made of a stainless steel cylinder enveloping a ceramic cylinder to provide mechanic strength and electronic insulation under high-pressure conditions. Two stainless steel pistons were used to press the sample and to serve as electronic connectors. The test cell was placed in a press (Carver Laboratory Press, Fred Carver Inc.) and the electrical resistance was measured by a milliohmmeter (Hewlett Packard, model 4328A). The electrical resistivity of carbon supports, FeTMPP chelates and carbon supported FeTMPP-Cl catalysts were measured under different pressures at room temperature. The cell with sample of FeTMPP-Cl on RB carbon was tested by using a SI 1260 Impedance/Gain-Phase analyzer and a SI 1287 Electrochemical Interface (Solartron Instruments Inc.) to examine if there is an interfacial resistance associated with the resistivity measurements.

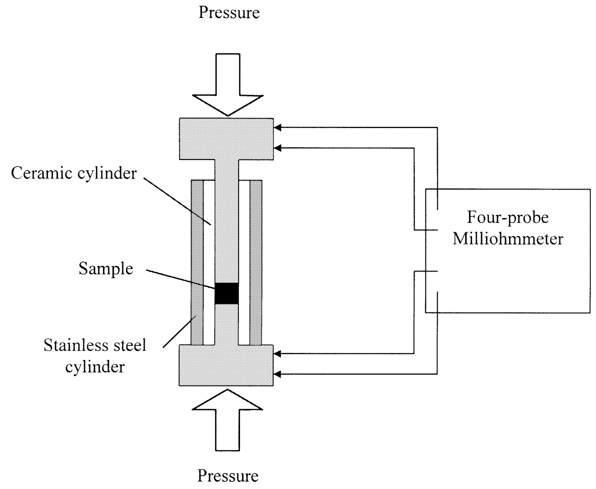

Fig. 1. Schematic of test hardware for four-probe electronic conductivity measurement.

2.4. *FTIR measurement*

Fourier transform infrared spectroscopy (FTIR) was performed with a Bomem MB100 FTIR single-beam apparatus equipped with a high intensity SiC source and a liquid-nitrogen cooled mid band MCT detector. Samples for FTIR experiment were prepared as potassium bromide (KBr) pellets with a concentration of 0.1 wt %. All catalysts and KBr were dried at specific temperatures in vacuum oven for overnight, separately. The catalyst and KBr were mixed and grinded with an agate mortar and pestle for about 5 min. The resulting mixture was then squeezed to produce a transparent pellet using a pressure of $(10\text{–}15) \times 10^5$ kPa.

2.5. *X-ray photoelectron spectroscopy*

Surface analysis of the FeTMPP-Cl/C catalysts with or without heat-treatment have been performed by X-ray photoelectron spectroscopy (XPS) on a 5600 ESCA system including a conventional dual anode X-ray source (Mg and monochromated Al) and a 20 inch hemispherical electron energy analyser. The AlK_α line at 1486.6 eV has been used for all samples. The core level spectra were calibrated by setting up the C1s peak. Powder samples prepared were fixed on a double-side adhesive carbon tape. The vacuum in the analysis chamber was in the region of 10^{-10} torr. Photoelectron spectra were recorded for the C_{1s}, Fe $2p_{3/2}$, N_{1s} and O_{1s} spectral regions. All spectra were referenced to the C_{1s} level of the carbon black at 284.35 eV.

A semi-quantitative analysis of the XPS data was performed using the relation $C_x = (I_x S_x)/\sum(I_I S_I)$ where C_x, S_x and I_x are the surface concentration, the area under the elemental XPS peak and sensitivity factor for the element ‘x’ [19].

2.6. *Elemental analysis*

The elemental analysis of the samples, such as FeTMPP-Cl without heat treatment, BP carbon supported FeTMPP-Cl catalyst and BP 2000 support before and after heat treatment, were performed at Galbraith Laboratories (Knoxville, TN).

2.7. *Fuel cell tests*

Polybenzimidazole (Celanese) films doped with approximately five phosphoric acid molecules per polymer repeat unit was used as electrolyte for the DMFC tests. The electrodes were prepared using a thin electrode technique [2]. The membrane/electrode (MEA) assemblies were formed by hot pressing the electrodes on an acid doped PBI membrane at 150 °C, 2.2×10^4 kPa for 10 min. The MEA assemblies were then impregnated by adding a few microlitres of 5 M H_3PO_4 solution on the gas backing side, and allowing the acid solution to penetrate into the electrode structure. The electrochemical experiments for fuel cell tests were carried out in a single cell test station as described in [2] at 150 °C and atmospheric pressure. Gas humidification was achieved by bubbling the gases through distilled water at room temperature. A liquid mixture with 1:2 molar ratio of methanol to water was used as anode feed and the cell resistance between anode and cathode was measured using the current interrupt method.

3. Results and discussion

3.1. *Specific surface area*

Figure 2 shows the specific surface area of the RB carbon and FeTMPP-Cl catalysts supported on RB carbon. These results were obtained by BET measurements. Each sample was measured three times, and the standard deviations of measurements were less than 2%. Figure 2 clearly shows that the specific surface area of the FeTMPP-Cl catalysts linearly decreases with increasing FeTMPP-Cl loading on RB carbon. Figure 2 also shows that the heat treatment at high temperature has no significant effect on the specific surface area for RB carbon substrate. One of the possible explanations for the decrease surface area with loading is that the chemical bonds between the carbon substrate and the FeTMPP chelate, or the fragments of the chelate after heat treatment at high temperature, were formed so that the surface of the carbon is occupied by the FeTMPP chelate or the fragments of the chelate. The other explanation is that the coverage of the FeTMPP-Cl on carbon blocked the pores in porous structure of the carbon, which results in the decrease of the specific surface area.

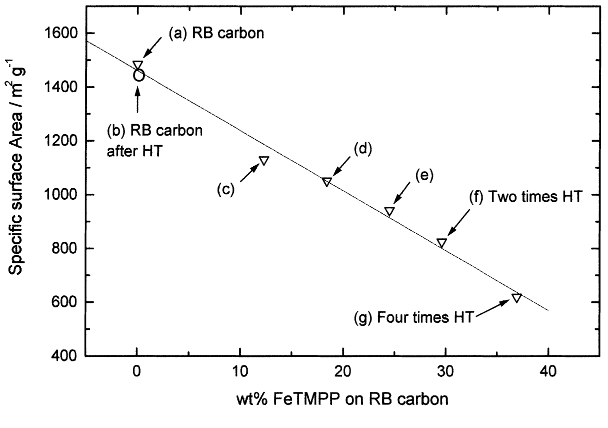

Fig. 2. Specific surface areas of (a) RB carbon, (b) RB carbon, one time HT at 800 °C, (c) 12.3 wt % FeTMPP on RB carbon, one time HT at 800 °C (d) 18.4 wt % FeTMPP on RB carbon, one time HT at 800 °C (e) 24.5 wt % FeTMPP on RB carbon, one time HT at 800 °C (f) 29.6 wt % FeTMPP on RB carbon, two times HT at 800 °C (g) 36.9 wt % FeTMPP on RB carbon, four times HT at 800 °C.

3.2. *Resistivity measurement*

It is known that FeTMPP-Cl is not a good electronic conductor. The high FeTMPP-Cl loading on RB carbon may cause a high electronic resistivity for the carbon supported FeTMPP-Cl catalysts. In order to explore this issue, the electronic resistivity of RB carbon and RB carbon supported FeTMPP-Cl catalysts that have different loading levels were measured by a four-probe millilohmmeter. As shown in Figure 3, it can be seen that the specific resistance is a function of the pressure. However, it approaches a constant value when the applied pressure is higher than 500 MPa. To verify the effectiveness of the test hardware, the cell with a sample of 12.3 wt % FeTMPP-Cl on RB carbon was measured by using an a.c. impedance system. The results are shown in Figure 4. This result clearly demonstrates a purely resistive behavior when the frequency is lower than 1 kHz. An inductive behaviour observed at high frequency is due to the stainless steel pistons that make connection to the sample. This suggests that, except for the electronic contact resistance, the resistance data are valid if the measuring frequency is lower than 1 kHz.

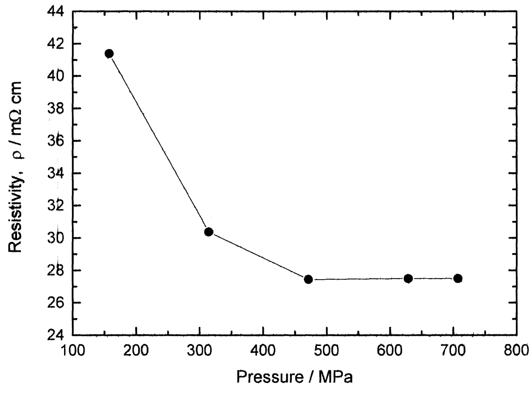

Fig. 3. Specific electrical resistance of uncatalysed RB carbon without heat-treatment measured at room temperature.

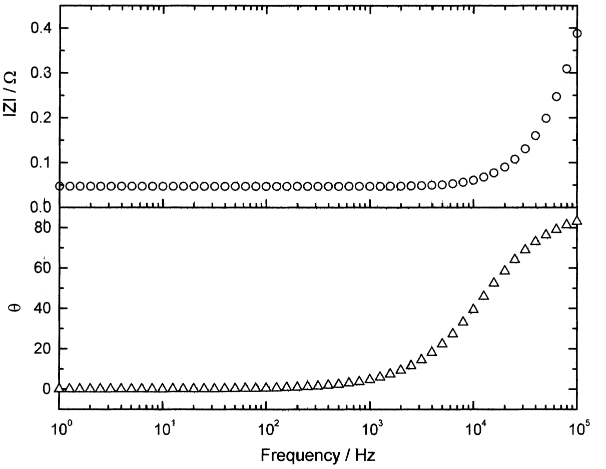

Fig. 4. A.c. impedance spectrum of 12.3 wt % FeTMPP on RB carbon. Pressure applied to electrodes 500 MPa cm^{-2}.

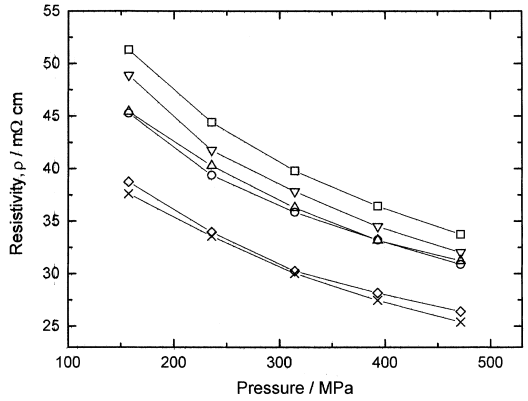

Fig. 5. Electrical resistivity of RB carbon with (○) and without (□) heat treatment at 800 °C. RB carbon supported FeTMPP-Cl catalysts treated at 800 °C for different loadings: (△) 12.3%, one time HT; (▽) 18.4%, one time HT; (◇) 29.6%, two times HT; (×) 36.9%, four times HT.

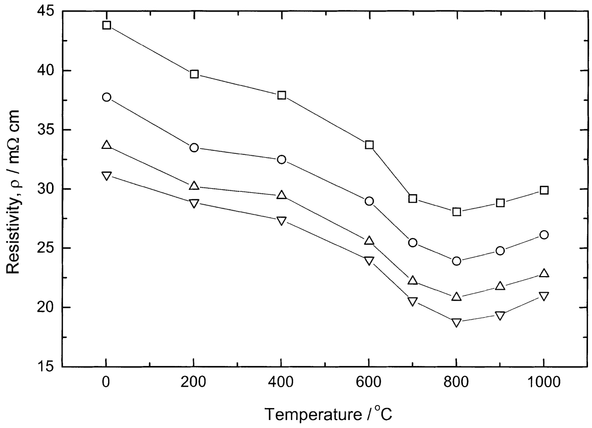

Fig. 6. Effect of heat treatment temperatures on the electrical resistivity for the sample of 24 wt % FeTMPP on RB carbon. Pressure: (□) 236, (○) 314, (△) 393 and (▽) 472 MPa.

The resistivity of carbon and catalyst samples measured are summarized in Figure 5. The resistivity of the RB carbon was lowered after heat-treated twice. This trend is also reflected in FeTMPP-Cl RB carbon supported catalyst samples, that is, the more heat-treatment given the sample, the more conductive the sample. There is no clear trend between the FeTMPP-Cl loading and the resistivity of the catalysts, as shown in Figure 5. The resistivity of the 18.4 wt % FeTMPP-Cl on RB carbon is higher than that of 12.3 wt % FeTMPP-Cl on RB carbon, however the resistivity of 29.6 and 36.9 wt % FeTMPP-Cl on RB carbon are lower than that of 12.3 wt % FeTMPP-Cl on RB carbon.

The effect of heat treatment temperature on the resistivity of the catalysts was also examined. Figure 6 displays the effect of the heat treatment temperature on the resistivity for samples of 24 wt % FeTMPP-Cl on RB carbon. The resistivity of the catalyst decreases as the heat-treatment temperature increases from 200 to 800 °C. Beyond 800 °C, a small increase in resistivity was observed, although it is not clear if this is due to the support or the macrocycles. A broad minimum occurs between 600–1000 °C. The results are in agreement with the literature [10, 15], in which Fe(II)TMPP catalysts prepared with heat treatment temperatures ranging from 600 to 1000 °C show good catalytic activity with the best activity obtained after a 800 °C heat treatment. However, it should be pointed out that the nonlinear relationship between the resistivity of catalysts and heat treatment temperature probably indicates different chemical processes taking place at different heat treatment temperatures.

3.3. *Elemental analysis*

The results of elemental analysis of the samples are shown in Table 1. It can be seen that the bulk concentration of iron in the BP carbon before and after heat treatments was in the level of less than 100 ppm and there is about one percent of nitrogen in the carbon. For the sample of BP 2000 carbon supported FeTMPP-Cl catalyst without heat treatment, the weight percentage of iron was almost the same as that of nitrogen after deducting the amount of nitrogen on the heat-treated BP 2000 carbon. This suggests that the molar ratio of iron to nitrogen is 1 to 4 and FeN_4 structural unit exists as in the case of the unsupported FeTMPP chelate. In

Table 1. Elemental composition in wt % of several carbon and catalyst samples

Sample	Iron	Nitrogen	Carbon	Hydrogen
BP 2000 carbon, no HT	∠92 ppm	1.03%		
BP 2000 carbon, HT at 800 °C	∠100 ppm	0.99%		
FeTMPP-Cl/BP 2000, no HT	1.29%	2.32%		
FeTMPP-Cl/BP 2000, HT at 800 °C	1.63%	1.59%		
FeTMPP-Cl, no HT	7.8%	7.7%	68.86%	5.77%

contrast, for the FeTMPP-Cl supported on BP 2000 carbon after heat treatment at 800 °C, the molar concentration of iron was much higher than that of nitrogen after deducting the amount of nitrogen on the heat-treated BP 2000 carbon. This indicates that more than a half of the nitrogen in the chelate disappears during the heat-treated process.

3.4. *FTIR spectra*

FTIR is a useful and direct technique for the study of the nature of oxygen-containing surface groups. However, there are well-know experimental difficulties involved in obtaining carbon spectra. There is also a common consensus on the fact that the interpretation of the surface groups on carbon is a difficult task since it is unrealistic to consider these groups as isolated functions like in classic organic chemistry [20]. FTIR adsorption spectra on dilute catalyst samples in KBr pellets are shown in Figures 7 and 8. It should be pointed out that the spectra only provide a qualitative comparison.

Figure 7 includes the spectra of (a) FeTMPP-Cl, (b) BP 2000 carbon after heat treatment at 800 °C and (c) FeTMPP-Cl supported on BP carbon. For the spectrum of FeTMPP-Cl (Figure 7(a)), all of the features occurring at wave-number region from 1660 cm^{-1} to 560 cm^{-1} were essentially identical to those reported earlier by Thomas and Martell [21] excepting two bonds at 874 and 893 cm^{-1} were not observed, which are assigned to the Fe–O–Fe stretching vibration modes for the $(\mathrm{FeTMPP})_2\mathrm{O}$ chelate [22, 23].

For the sample of BP 2000 carbon support, the spectrum in the 1670–1500 cm^{-1} region in Figure 7(b) were overlapped by several absorption bands. The bands appearing in this region have not been interpreted unambiguously by different authors. The most common interpretation given to absorption in this frequency range has been related to C=C stretching vibration of surface groups on the carbon. Studebacker [24] assigned the region 1675–1550 cm^{-1} to quinone structures. Zawadzki [25] attributed an absorption band at 1590 cm^{-1} in carbonized films of polyfurfuryl alcohol and cellulose, together with overlapping bands in the region of 1500–1100 cm^{-1} to thermal stable carboxyl-carbonate structure. Two large absorption bands centered at 1580 and 1049 cm^{-1} can be assigned to carboxylic groups, quinonic or aromatic ethers with a variable distribution from one type of support to the other [26]. The bands in 1100–1000 cm^{-1} region may be associated with acidic surface groups. This region is characteristic of C–O stretching vibrations.

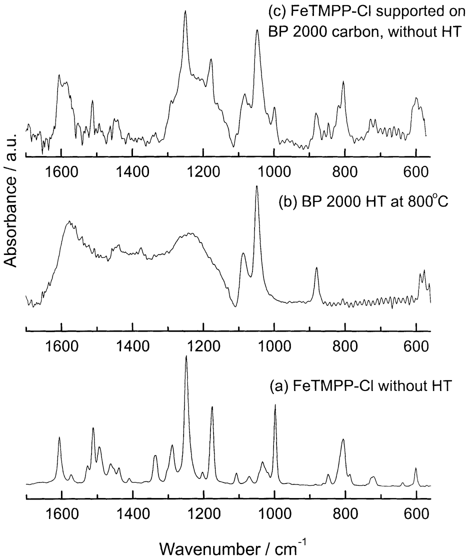

Fig. 7. FTIR spectra for the samples of (a) FeTMPP without HT, (b) BP 2000 carbon support HT 800, (c) BP 2000 carbon supported 24 wt % FeTMPP without HT.

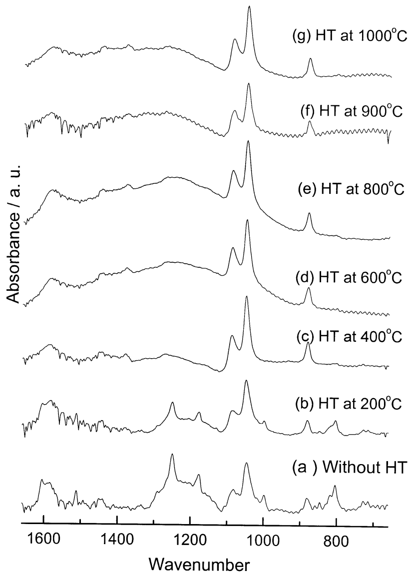

Fig. 8. FTIR spectra for the samples of 24 wt % FeTMPP supported on BP 2000 carbon (a) without HT, (b) HT 200, (c) HT 400, (d) HT 600, (e) HT 800, (f) HT 900 (g) HT 1000.

The spectrum of BP 2000 carbon supported FeTMPP-Cl catalyst (Figure 7(c)) appears qualitatively as an overlap generated by the BP 2000 carbon spectrum and the FeTMPP-Cl spectrum. This clearly visible combined spectrum indicates that the molecular structure of FeTMPP-Cl was still intact on the carbon as its precursor, and it is possible to use FTIR technique for studying the configuration of the carbon supported FeTMPP-Cl.

Figure 8 exhibits the spectra of BP 2000 carbon supported FeTMPP-Cl catalysts after heat treatment at various temperatures. In the cases of samples (a) and (b), the molecule of FeTMPP-Cl was intact on the carbon and equivalent to its precursor. However, for samples (c) to (g) with heat treatment temperatures ranging from 400 to 1000 °C, most features characterizing the organic groups of the chelate have disappeared. Obviously, the concentration of the FeTMPP-Cl decreases below the level of detection, which suggests that the molecular structure of FeTMPP-Cl on the carbon is destroyed by heat treatment at the temperatures higher than 400 °C. This result is consistent with that of pyrolysis-mass spectrometry studies (7) and other studies [14], where it was observed that the onset temperature for partial decomposition occurred at temperatures of about 400–500 °C for this macrocycle either as crystals or dispersed on high area carbon. It is interesting to note that the spectra for the sample (c) to (g) are very similar to the spectrum of BP carbon support.

3.5. *X-ray photoelectron spectroscopy*

The XPS spectra of BP 2000 carbon supported Fe-TMPP-Cl catalysts heat-treated at various temperature were obtained for the Fe2p$_{3/2}$, Nls and Ols, respectively. The result of semi-quantitative analysis for surface concentration in atoms is listed in Table 2. In Table 2, the surface concentrations of iron were low for the samples without heat treatment (a) and with heat-treated at 200 °C (b). A maximum iron surface concentration appears to occur in the range of 400–800 °C. For the sample heat-treated at 1000 °C, no clearly visible peak at the approximate binding energy of 710 eV was observed. On the other hand, by comparing concentration in Table 1 and Table 2, the concentration of iron on the surface was much lower than that of in the bulk. For example, for 0.24 at % Fe on carbon, this corresponds to approximately 1.1 wt % as compared 1.63 wt % from bulk analysis. The possible reason for this observation is that most of the iron was encapsulated by carbon in the process of catalyst thermal treatment [14]. The surface content of iron on carbon within the depth of 10 nm was very low for the samples without heat treatment (a) and with heat-treated at 200 °C (b). Upon increasing the heat treatment temperature, the sublimation and subsequent redeposition of the chelates (eventually followed by their fragments) occurs on the carbon surface. These fragments will likely be more evenly spread on the carbon surface. The flowing argon might remove some of the fragments resulting from partial decomposition of organic groups in the FeTMPP chelate. Consequently, the surface concentration of iron-containing compounds or fragments contributes to enhancing catalyst conductivity as described above. Beyond 800 °C, the surface concentration of iron decreases significantly. This observation may be related to the appearance of metallic iron clusters with dimension exceeding the escape range of the X-ray generated Fe2p photoelectrons. Since the size of the metallic clusters increases with heat treatment temperature, the increasing number of metallic atoms become undetectable so that the surface concentration of iron appears to decline. Other authors [10, 27] also observed this behavior.

Table 2. Surface concentration of iron, nitrogen and oxygen, at % on BP 2000

Sample	Heat-treated temperature	Iron	Nitrogen	Oxygen
a	No HT	0.18 ± 0.02	0.98 ± 0.02	3.25 ± 0.02
b	200 °C	0.17 ± 0.02	0.92 ± 0.02	3.89 ± 0.02
c	400 °C	0.23 ± 0.02	1.13 ± 0.02	3.72 ± 0.02
d	600 °C	0.25 ± 0.02	1.17 ± 0.02	1.68 ± 0.02
e	700 °C	0.27 ± 0.02	1.22 ± 0.02	2.53 ± 0.02
f	800 °C	0.24 ± 0.02	0.99 ± 0.02	2.85 ± 0.02
g	1000 °C	0.08 ± 0.02	0.36 ± 0.02	2.98 ± 0.02

Table 2 shows that the surface concentration of nitrogen on carbon behaves in a way similar to the surface concentration of iron. It should be noted that the surface concentrations of nitrogen are four times in atoms more as those of iron. This implies that the FeN$_4$ structural unit still remains on the carbon at the heat treatment temperatures below 800 °C. This, of course, is in contrast to bulk analysis shown in Table 1 and an explanation is not obvious.

The iron oxide formation can easily be interpreted considering the high oxygen content present on the surface of the carbon structure in Table 2. However, owing to the weak satellite intensity of the Fe2p$_{3/2}$ spectra, oxygen atoms seem to be bonded not only to iron atoms but also to other atoms such as nitrogen and carbon etc.

3.6. *Fuel cell tests*

The cathodic performance of a H_2/O_2 and CH_3OH/O_2 PBI fuel cell with a FeTMPP-Cl cathode is shown in Figure 9. The catalyst used was 17.6 wt % FeTMPP-Cl supported on RB carbon which was heat-treated at 800 °C in argon. The electrode structure was not optimized in terms of the catalyst loading and PBI polymer loading, as well as the process of fabricating electrodes and MEA assembly. Figure 9 demonstrated that the cathodic performance was nearly unaffected by switching hydrogen to methanol for the anode feed.

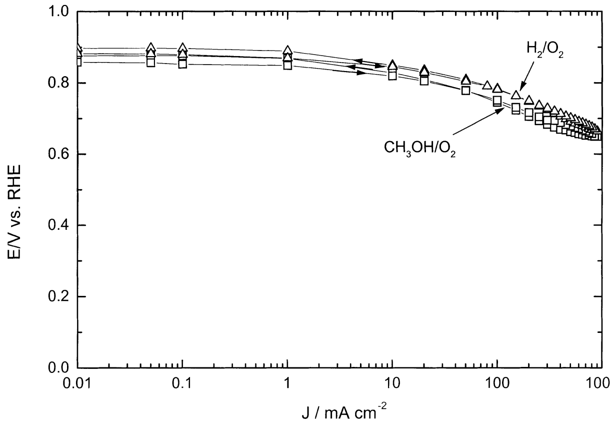

Fig. 9. Cathode performance of 18.4 wt % FeTMPP-Cl on RB carbon for oxygen reduction. Electrode composition: 1.5 mg cm^{-2} FeTMPP-Cl/C with 1.8 mg cm^{-2} PBI, humidified O_2. PBI membrane doped with 500 mol % H_3PO_4. Anode side was fed with 1 atm H_2 humidified at room temperature for H_2/O_2 or a liquid mixture with 1:2 molar ratio of methanol to water for CH_3OH/O_2. Cell temperature: 150 °C.

Thus methanol tolerant behavior for the catalyst is clearly demonstrated.

4. Summary

The physical and chemical properties of carbon supported FeTMPP-Cl/C catalysts before and after heat treatment were investigated by measuring specific surface area, catalyst electronic resistivity, and performing elemental analysis, FTIR and XPS spectroscopy studies. The results demonstrate that the onset temperature for partial decomposition for the FeTMPP chelate occurs at temperatures of about 400–500 °C. Beyond this temperature, it appears that molecular structure of FeTMPP chelate on carbon is destroyed by the heat treatment. The surface concentrations of both iron and nitrogen on the carbon increase with increasing heat treatment temperature, and a broad maximum occurs at temperature of around 400–800 °C. It is suggested that iron-containing compounds or fragments are formed on carbon surface at the high temperatures. Consequently, the resistivity of the catalysts shows a minimum at the same temperature region. Fuel cell test indicates that the catalyst behaves as methanol tolerant.

Acknowledgement

This work was supported under a University Research Initiate Grant from the Advanced Research Projects Agency, ONR grant N00014-92-J-1848.

References

1. M. Wilson and S. Gottesfeld, *J. Appl. Electrochem.* **22** (1992) 1.
2. J.-T. Wang, R.F. Savinell, J. Wainright, M. Litt and H. Yu, *Electrochim. Acta* **41** (1996) 193.
3. R. Jasinski, *Nature* **201** (1964) 1212.
4. H. Jahnke, M. Schonborn and G. Zimmerman, *Fortschr. Chem. Forsch.* **61** (1976) 133.
5. A.B. Hoffman, D.M. Collins, V.W. Day, E.B. Fleischer, T.S. Srivastava and J.L. Hoard, *J. Amer. Chem. Soc.* **94** (1972) 3620.
6. D. Scherson, S.L. Gupta, C. Fierro, E.B. Yeager, M.E. Kordesch, J. Eldridge, R.W. Hoffman and J. Blue, *Electrochim. Acta* **28** (1983) 1205.
7. D. Scherson, A.A. Tanaka, S.L. Gupta, D. Tryk, C. Fierro, R. Holze and E.B. Yeager, *Electrochim. Acta* **31** (1986) 1247.
8. K. Wiesener, *Electrochim. Acta* **31** (1986) 1073.
9. A. Biloul, P. Gouerec, M. Savy and G. Scarbeck, *J. Appl. Electrochem.* **26** (1996) 1139.
10. G. Faubert, G. Lalande, R. Cote, D. Guay, J.P. Dodelet, L.T. Weng, P. Bertrand and G. Denest, *Electrochim. Acta* **41** (1996) 1689.
11. G. Lalande, R. Cote, D. Guay, J.P. Dodelet, L.T. Weng and P. Bertrand, *Electrochim. Acta* **42** (1997) 1379.
12. J.A.R. van Veen, J.F. van Baar and K.J. Kroese, *J. Chem. Soc. Faraday Trans.* **77** (1981) 2827.
13. J.A.R. van Veen, H.A. Colijn and J.F. van Baar, *Electrochim. Acta* **33** (1988) 801.
14. S.Lj. Gojkovic, S. Gupta and R.F. Savinell, *J. Electrochem. Soc.* **145** (1998) 3493.
15. S.Lj. Gojkovic, S. Gupta and R.F. Savinell, *J. Electronal. Chem.* **462** (1999) 63.
16. S.Lj. Gojkovic, S. Gupta and R.F. Savinell, *Electrochim. Acta.* **45** (1999) 899.
17. G.Q. Sun, J.T. Wang and R.F. Savinell, *J. Appl. Electrochem.* **28** (1998) 1087.
18. S. Gupta, D. Tryk, S.K. Zecevic, W. Aldred, D. Guo and R.F. Savinell, *J. Appl. Electrochem.* **28** (1998) 673.
19. D. Briggs and M.P. Seah, 'Practical Surface Analysis by Auger and X-ray Photoelectron Spectroscopy' (J. Wiley & Sons, New York, 1983).
20. E. Papirer and E. Guyon, *Carbon* **16** (1978) 127.
21. D.W. Thomas and A.E. Martell, *J. Am. Chem. Soc.* **81** (1959) 5111.
22. E.T. Shimomura, M.A. Phillippi and H.M. Goff, *J. Am. Chem. Soc.* **103** (1981) 6778.
23. I.A. Cohen, *J. Am. Chem. Soc.* **91** (1969) 1980.
24. M.L. Studebaker and R.W. Rinehart, Jr., *Rubber Chem. Technol.* **45** (1972) 106.
25. J. Zawadzki, *Carbon* **16** (1978) 491.
26. K.A. Radyushkina, *J. Res. Inst. Catal.* **30** (1982) 155.
27. M. Ladouceur, G. Lalande, D. Guay, J.P. Dodelet, L. Dognard-Bailey, M.L. Trudeau and R. Schulz, *J. Electrochem. Soc.* **140** (1993) 1974.